Vacuum induced torque between corrugated metallic plates

Robson B. Rodrigues[1], Paulo A. Maia Neto[1] (*), A. Lambrecht[2] and S. Reynaud[2] (**)

[1] *Instituto de Física, UFRJ, Caixa Postal 68528, 21941-972 Rio de Janeiro RJ, Brazil*
[2] *Laboratoire Kastler Brossel, CNRS, ENS, UPMC case 74, Campus Jussieu, 75252 Paris, France*

Abstract. – We study the torque arising between two corrugated metallic plates due to the interaction with electromagnetic vacuum. This Casimir torque can be measured with torsion pendulum techniques for separation distances as large as $1\mu m$. It allows one to probe the nontrivial geometry dependence of the Casimir energy in a configuration which can be evaluated theoretically with accuracy. In the optimal experimental configuration, the commonly used proximity force approximation turns out to overestimate the torque by a factor 2 or larger.

The Casimir effect [1] plays a major role in micro- and nano-electromechanical systems (MEMS and NEMS) [2]. Besides the normal Casimir force between metallic or dielectric plates [3], the observation of the lateral Casimir force between corrugated plates [4] opens novel possibilities of micro-mechanical control. The lateral force results from breaking the translational symmetry along directions parallel to the plates by imprinting periodic corrugations on both metallic plates. As rotational symmetry is also broken by this geometry, a Casimir torque should also arise when the corrugations are not aligned. In the present letter, we study this effect which provides one with a new mechanism of micro-mechanical control to be exploited in the design of MEMS and NEMS.

From the point of view of fundamental physics, this effect makes possible an accurate investigation of the non-trivial geometry dependence of the Casimir energy. Tests of this geometry dependence performed up to date have often been limited by the use of the proximity-force approximation (PFA) in the calculations [5]. Within this approximation, the energy is evaluated by simply averaging the Casimir energy between two planes over the distribution of local distances, which is certainly insufficient except for the limiting case of large corrugation wavelengths [6]. Other calculations [7] have gone farther than PFA while using a model of perfect reflection, which limited their validity to experiments performed with metallic mirrors at distances larger than a few μm.

Here we use the scattering approach [8, 9] extended to treat non-planar surfaces [10, 11]. This perturbative approach is restricted by the assumption that corrugation amplitudes are

smaller than other length scales but it allows one to go beyond the range of validity of the PFA, with arbitrary values of the corrugation wavelengths with respect to plate separation and plasma wavelength of the metal. As shown below, it accurately describes configurations which are experimentally testable and where the Casimir energy has a non-trivial geometry dependence. This new effect induced by vacuum fluctuations may be small because the corrugation amplitudes are small, but the torque detection is particularly interesting from this point of view, since it allows one to use the exquisite sensitivity of torsion balances [12].

The idea of using torsion techniques has already been proposed to measure Casimir torques between anisotropic dielectric plates [13–16]. Recently, an experiment has been proposed to measure the torque with a birefringent disk on top of a barium titanate plate [17]. According to the authors, the proposed measurement is feasible at a plate separation L of 100nm. We show below that the torque between corrugated metallic plates is up to three orders of magnitude larger than the torque between anisotropic dielectric plates, for comparable values of the separation distance and plate area. With realistic values for the corrugation amplitudes a_1 and a_2 and wavelength λ_C, we conclude that the torque measurement may be done at a distance L of the order of 1μm. This minimizes the spurious effects due to the non-parallelism of the plates while making the contribution of interband transitions negligible. We thus model the finite conductivity of the metallic plates by the plasma model with a plasma wavelength λ_P. We calculate the modification of the Casimir energy up to second order in the corrugation amplitudes assumed to be smaller than other length scales

$$a_1, a_2 \ll L, \lambda_C, \lambda_P \tag{1}$$

This condition, allowing us to use perturbation theory, will be satisfied by the numerical examples discussed below.

The surface profile functions for the two plates are denoted as $h_j(\mathbf{r})$ with $j = 1, 2$ labeling the two plates. They define the local heights, counted as positive when corresponding to separation decreases with respect to reference planes at $z = 0$ and $z = L$. Both h_j have zero spatial averages, so that L represents the average separation distance between the two surfaces, and $\mathbf{r} = (x, y)$ collects the two transverse coordinates defining the position on the plates. The corrugated surfaces are described by non-specular reflection coefficients that couple different field polarizations and momenta [18]. The second-order correction is then given by [11]

$$\delta E_{\mathrm{PP}} = \int \frac{d^2\mathbf{K}}{(2\pi)^2} \mathcal{G}(\mathbf{K}) H_1(\mathbf{K}) H_2(-\mathbf{K}), \tag{2}$$

where $H_j(\mathbf{K})$ is the Fourier transform of $h_j(\mathbf{r})$. The response function $\mathcal{G}(\mathbf{K})$ does not depend on the direction of the corrugation wavevector $\mathbf{K}$. It is given in [11] as a function of the specular and non-specular reflection coefficients. Only the crossed terms of the form $H_1 H_2$ are kept in eq. (2), since terms quadratic in H_1 and in H_2 do not depend on the relative angle between the plates, and hence do not contribute to the torque.

We assume the corrugations to have sinusoidal shapes $h_j(\mathbf{r}) = a_j \cos(\mathbf{k}_j \cdot \mathbf{r} - kb_j)$ with corrugation wavevectors $\mathbf{k}_j$ having the same modulus $k = 2\pi/\lambda_C$. The angle θ between $\mathbf{k}_1$ and $\mathbf{k}_2$ represents the angular mismatch between the two corrugations and $\mathbf{k}_2$ is supposed, for convenience, to be aligned along the direction of the $x-$axis. The parameters b_j represent lateral displacements with respect to the configuration with a line of maximum height at the origin. With these conventions, eq. (2) yields

$$\delta E_{\mathrm{PP}} = a_1 \, \mathcal{G}(k) \, \mathrm{Re} \left[e^{ikb_1} H_2(\mathbf{k}_1) \right] \tag{3}$$

The integral yielding $H_2(\mathbf{k}_1)$ may be specified by considering that the corrugation h_2 is restricted to a rectangular section of area $L_x L_y$ centered at $x = b_2, y = 0$. We assume that both L_x and L_y are much larger than L, so that diffraction at the borders of the plates is negligible. The energy correction per unit area is then given by

$$\frac{\delta E_{\text{PP}}}{L_x L_y} = \frac{a_1 a_2}{2} \mathcal{G}(k) \cos{(kb)} \text{sinc}(kL_y \sin \theta/2) \sum_{\epsilon=\pm} \text{sinc}\left[kL_x(1 + \epsilon \cos \theta)/2\right] \tag{4}$$

$$b = b_2 \cos \theta - b_1 \quad, \quad \text{sinc}(x) \equiv \frac{\sin(x)}{x} \tag{5}$$

b is the relative lateral displacement along the direction of $\mathbf{k}_1$; as expected by symmetry, the energy does not depend on displacements perpendicular to $\mathbf{k}_1$. Eq. (4) satisfies reflection symmetry around the x and y directions (invariance under the transformations $\theta \to -\theta$ and $\theta \to \pi - \theta$), which results from the fact that the corrugation lines have no orientation. It contains as a special case ($\theta = 0$) the result for pure lateral displacement derived in Ref. [11].

The energy variation with b and θ given by eq. (4) is universal, since the separation distance L and additional parameters characterizing the metallic surfaces determine only the global pre-factor $\mathcal{G}(k)$. In the limit of long corrugation lines, $kL_y \gg 1$, we may take the approximation $\theta \ll 1$ in eq. (4), since δE_{PP} is negligible otherwise. If L_x is smaller or of the order of L_y, we find from eq. (4)

$$\frac{\delta E_{\text{PP}}}{L_x L_y} = \frac{a_1 a_2}{2} \mathcal{G}(k) \cos{(kb)} \text{sinc}(kL_y \theta/2). \tag{6}$$

Hence, the scale of variation of θ is set by the parameter $1/(kL_y) = \lambda_C/(2\pi L_y)$.

In Fig. 1, we plot δE_{PP} (in arbitrary units) as a function of b and θ. Since $\mathcal{G}(k)$ is negative [11], the Casimir energy is minimum at $\theta = 0$ and $b = 0, \lambda_C, 2\lambda_C, ...$, corresponding to the geometry with aligned corrugations and the local separation distance having the maximum variation amplitude. There are also shallow wells around $\theta \approx 1.43 \lambda_C/L_y$ (minimum of $\text{sinc}(kL_y \theta/2)$) and $b = \lambda_C/2, 3\lambda_C/2, ...$ If we start from $\theta = b = 0$ and rotate plate 2 around its center, we follow the line $b = 0$ in Fig. 1. This figure shows that for small angles the plate is attracted back to $\theta = b = 0$ without sliding laterally. On the other hand, if the plate is released after a rotation of $\theta > \lambda_C/L_y$ its subsequent motion will be a combination of rotation and lateral displacement. In fact, the energy correction vanishes at $\theta = \lambda_C/L_y$, defining the range of stability of the configuration $b = \theta = 0$. Rotation is favored over lateral displacements for $\theta < \lambda_C/L_y$.

We now proceed to an evaluation of the torque which is given by

$$\tau = -\frac{\partial}{\partial \theta} \delta E_{\text{PP}}. \tag{7}$$

It is maximum at $\theta = 0.66 \lambda_C/L_y$ where it is given by

$$\frac{\tau}{L_x L_y} = 0.109 \, a_1 a_2 \, k\mathcal{G}(k) \, L_y. \tag{8}$$

As could be expected, this maximal torque per unit area is proportional to the length L_y of the corrugation lines, which provides the scale for the moment arm. In order to plot the value of the torque (8) on Fig. 2, we take the plasma wavelength corresponding to gold for both plates ($\lambda_P = 137$nm). We chose corrugation amplitudes $a_1 = a_2 = 14$ nm obeying condition (1) and leading to $a_1 a_2 = 200$ nm^2 (to be compared with $a_1 a_2 = 472$ nm^2 in the lateral force experiment [4], where a_1 and a_2 were unequal) and $L_y = 24 \, \mu$m. Different values for $a_1 a_2$ and
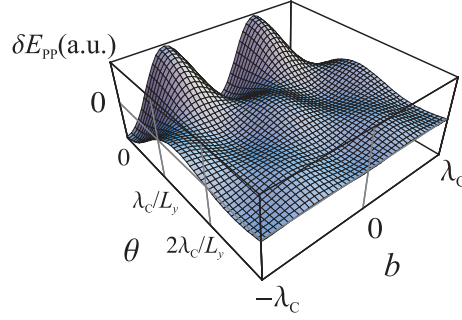
Fig. 1 – Variation of Casimir energy (in arbitrary units) with the rotation angle θ and the lateral displacement b.

L_y can also be derived from these results through a mere multiplication by suitable pre-factors (see eq. 8), provided that these values satisfy $a_1, a_2 \ll L, \lambda_C$ and $L_y \gg \lambda_C/(2\pi)$. The first condition is at the heart of our perturbative approach, whereas the second condition can be relaxed by going back to the more general result (4).

The dashed line in Fig. 2 corresponds to the corrugation period $\lambda_C = 1.2\,\mu$m of the lateral force experiment [4]. At $L = 100\,$nm, we find in this case $\tau/(L_x L_y) = 5.2 \times 10^{-7}\,$N.m^{-1}, approximately three orders of magnitude larger than the torque per unit area for anisotropic plates calculated in Ref. [17] for the most favorable configuration at the same separation distance. The much larger figures found in our case should certainly allow one to perform the experiment at larger separation distances. For $L \gtrsim 1\,\mu$m, Fig. 2 shows that the torque for $\lambda_C = 1.2\,\mu$m starts to decrease exponentially. However, by selecting longer corrugation periods, one also finds measurable orders of magnitude in this range of distances.

At any given value of L, the torque between corrugated plates can be made larger by chosing the corrugation period so as to maximize $k\mathcal{G}(k)$. In the range of separation distances shown on Fig. 2, this corresponds to $k \approx 2.6/L$ or $\lambda_C \approx 2\pi L/2.6$. The torque is thus given by the dotted line, which provides upper bounds for its magnitude. At $L = 1\,\mu$m, the optimum value is $\lambda_C = 2.4\,\mu$m, corresponding to the solid line in Fig. 2. In this case, we find $\tau/(L_x L_y) = 3.0 \times 10^{-12}\,$N.m^{-1}. As for the relevant angle scales, the stability threshold is at $\theta = \lambda_C/L_y = 0.1\,$rad $= 5.7^\circ$ and the maximum torque at $\theta = 3.8^\circ$. If rotation is to be observed from the position of the tip of the rectangular plate, then the relevant parameter is the arc described by the tip $(L_y/2)\theta \sim \lambda_C$, which is independent of L_y.

Under such optimum conditions, the torque probes a non-trivial geometry dependence of the Casimir energy, since the PFA thus grossly overestimates the effect, as shown now. The PFA holds for smooth surfaces corresponding to the limit $\lambda_C \to \infty$. It is recovered from eq. (8) at the limit $k \to 0$, where the response function satisfies the general condition [11] $\mathcal{G}(0) = e''_{\mathrm{PP}}(L)$, where e_{PP} is the Casimir energy per unit area for parallel planes. In this limit, the effect of geometry is trivial because the PFA directly connects the non-planar geometry to the more commonly studied configuration of parallel planes. We thus find a result determined by the Casimir energy for this simpler geometry:

$$\left(\frac{\tau}{L_x L_y}\right)_{\mathrm{PFA}} = 0.109\, a_1 a_2\, k e''_{\mathrm{PP}}(L)\, L_y. \tag{9}$$

In order to compare with the PFA, we plot our results for the torque as a function of k for $L = 1\,\mu$m in Fig. 3 (solid line), and with all other parameters as in Fig. 2. As discussed above,
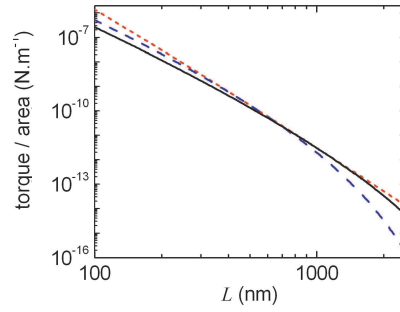
Fig. 2 – Maximum torque per unit area as a function of mean separation distance. Corrugation amplitudes: $a_1 a_2 = 200\,\mathrm{nm}^2$, line length: $L_y = 24\,\mu\mathrm{m}$, plasma wavelength: $\lambda_P = 137\,\mathrm{nm}$. Solid line: $\lambda_C = 2.4\,\mu\mathrm{m}$; dashed line: $\lambda_C = 1.2\,\mu\mathrm{m}$; dotted line: $\lambda_C = 2\pi L/2.6$ (optimum value).

the torque is maximum at $k = 2.6/L = 2.6\,\mu\mathrm{m}^{-1}$. We also show the values obtained from the model with perfect reflectors (dashed line). They overestimate the torque by 16% near the peak region.

According to eq. (9), the torque grows linearly with k in the PFA (dotted line). It is thus worth increasing the value of k and hence going out the region of validity of PFA. At the peak value $k = 2.6/L = 2.6\,\mu\mathrm{m}^{-1}$, the PFA overestimates the torque by 103%. As the torque decays for larger values of k, the PFA rapidly becomes less and less accurate. The discrepancy is measured by the ratio

$$\rho(k) = \frac{\mathcal{G}(k)}{e_{\mathrm{PP}}''(L)} = \frac{\mathcal{G}(k)}{\mathcal{G}(0)} \tag{10}$$

At $k = 0$, the exact and PFA values coincide ($\rho(0) = 1$). For $k > 0$, $\rho(k) < 1$, as in the numerical example of Fig. 4. Thus, the PFA always overestimates the torque and the discrepancy increases with k, as expected, since smaller values of k correspond to smoother surfaces.

For $k \gg 1/L$, $\mathcal{G}(k)$ and $\rho(k)$ decay exponentially to zero. Such behavior has a simple
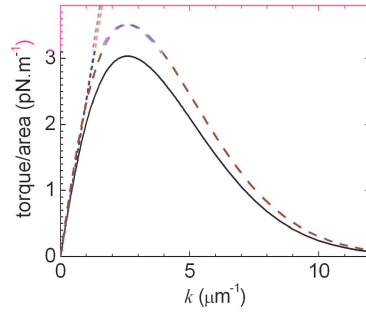

Fig. 3 – Maximum torque per unit area as a function of $k = 2\pi/\lambda_C$ with $L = 1\,\mu\mathrm{m}$. Additional parameters are chosen as in Fig. 2. The solid line corresponds to the theory presented in this letter. We also plot the results for perfect reflectors (dashed line) and PFA with plasma model (dotted line).
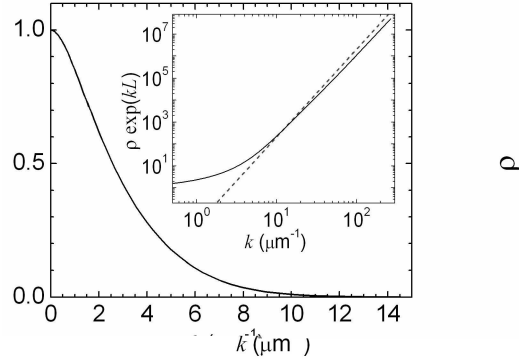
Fig. 4 – Variation of ρ versus k. Parameters are chosen as in Fig. 3. Inset: variation of $\rho(k)\exp(kL)$ (solid line) and perfectly-reflecting high-k limit (dashed line).

interpretation within the scattering approach [11]. The reflection by the corrugated surfaces produce lateral wavevector components of the order of k. After replacing the integral over real frequencies by an integral over the imaginary axis in the complex plane, we obtain propagation factors, representing one-way propagation between the plates, of the order of $\exp(-kL)$.

In order to analyze the large-k behavior in more detail, we plot $\rho(k)\exp(kL)$ in the inset of Fig. 4. In the intermediate range $1/L \ll k \ll 2\pi/\lambda_P = 46\,\mu\mathrm{m}^{-1}$, $\rho(k)$ approaches the high-k limit of the model with perfect reflectors [7], drawn as the dashed line in the inset of Fig. 4,

$$\rho(k) = \frac{2}{\pi^4}\,(kL)^4\,\exp(-kL) \qquad \text{(perfect reflectors)} \tag{11}$$

As k approaches $2\pi/\lambda_P$, $\rho(k)$ stays more and more below the result for perfect reflectors, reaching the following limit for very large values of k (not shown on the figure),

$$\rho(k) = \frac{5}{2}\,kL\,\exp(-kL) \qquad (1/L \ll 2\pi/\lambda_P \ll k) \tag{12}$$

Thus, the perfect-reflecting regime is reached only when the plasma wavelength is the shortest length scale in the problem (apart from the corrugation amplitudes). Just taking the limit $L \gg \lambda_P$ is not sufficient for recovering the limit of perfect reflectors [7]. This has again a very simple interpretation in the scattering approach. When $L \gg \lambda_P$, the relevant input field modes are perfectly reflected because they have wavevectors of order of $1/L$. However, diffraction by the corrugated surfaces produces wavevectors of the order of k, which are poorly reflected by the plates if $k \gg 1/\lambda_P$.

In conclusion, we have studied the torque induced by vacuum fluctuations between corrugated metallic plates. This Casimir torque may provide one with a new mechanism of micro-mechanical control to be exploited in the design of MEMS and NEMS. It could as well be a new observable of interest to test the geometry dependence of the Casimir energy. We recover the PFA from our theory in the limit $L \ll \lambda_C$, but deviations become rapidly important as L/λ_C is increased.

The torque is up to three orders of magnitude larger than the torque between anisotropic dielectric plates for comparable distance and area. This should allow for an experimental observation of the Casimir torque at separation distances around $L = 1\,\mu\mathrm{m}$, using corrugation

periods of the same order of magnitude ($\lambda_C = 2.4L$). In this configuration, the PFA grossly overestimates the torque by a factor of the order of 2. Moreover, it predicts an algebraic decay of the torque as L is increased past the optimum value, whereas the exact decay is actually exponential. This experiment would provide, for the first time, direct evidence of the nontrivial geometry dependence of the Casimir effect.

$$* * *$$

REFERENCES

[1]   CASIMIR H. B. G., *Proc. K. Ned. Akad. Wet.*, **51** (1948) 793.
[2]   CHAN H. B., AKSYUK V. A., KLEIMAN R. N., BISHOP D. J. and CAPASSO, F., *Science*, **291** (2001) 1941.
[3]   KLIMCHITSKAYA G. L. *et al*, *J. Phys. A: Math Gen.* **39** (2006) 6485 and references therein.
[4]   CHEN F., MOHIDEEN U., KLIMCHITSKAYA G. L. and MOSTEPANENKO V. M., *Phys. Rev. Lett.* **88** (2002) 101801; *Phys. Rev.* A **66** (2002) 032113.
[5]   DERIAGIN B. V., *Kolloid Z.* **69** (1934) 155; DERIAGIN B. V., ABRIKOSOVA I. I. and LIFSHITZ E. M., *Quart. Rev.* **10** (1968) 295.
[6]   GENET C., LAMBRECHT A., MAIA NETO, P. and REYNAUD S., *Europhys. Lett.* **62** (2003) 484 .
[7]   EMIG T., HANKE A., GOLESTANIAN R. and KARDAR M., *Phys. Rev.* A **67** (2003) 022114.
[8]   GENET C., LAMBRECHT A. and REYNAUD S., *Phys. Rev.* A **67** (2003) 043811.
[9]   LAMBRECHT A., MAIA NETO P. A. and REYNAUD S., submitted (2006).
[10] MAIA NETO, P. A., LAMBRECHT A. and REYNAUD S., *Phys. Rev.* A **72** (2005) 012115 .
[11] RODRIGUES R. B., MAIA NETO P. A., LAMBRECHT A. and REYNAUD S., *Phys. Rev. Lett.* **96** (2006) 100402.
[12] GUNDLACH J.H., *Meas. Sci. Technol.* **10** (1999) 454.
[13] PARSEGIAN V. A. and WEISS G. H., *J. Adhes.* **3** (1972) 259.
[14] BARASH Y., *Izv. Vyssh. Uchebn. Zaved., Radiofiz.* **12** (1978) 1637;.
[15] van ENK S. J., *Phys. Rev.* A **52** (1995) 2569.
[16] TORRES-GUSMÁN J. C. and MOCHÁN W. L., *J. Phys. A: Math Gen.* **39** (2006) 6791.
[17] MUNDAY J. N., IANNUZZI D., BARASH Y. and CAPASSO F., *Phys. Rev.* A **71** (2005) 042102.
[18] Whereas the method developed in Ref. [7] requires the existence of a direction of translational symmetry (so as to allow for the definition of field polarizations conserved in the scattering by the surfaces), our approach allows for the calculation in a geometry with no such symmetry, such as the rotated corrugated plates, because it explicitly takes into account the coupling between different polarizations.